Available online at www.sciencedirect.com
SCIENCE DIRECT®
Journal of Sound and Vibration 282 (2005) 863–880
JOURNAL OF SOUND AND VIBRATION
www.elsevier.com/locate/jsvi

Characteristic analysis of wave propagation in anisotropic fluid-saturated porous media

Ying Liu[a,*], Kaishin Liu[a], Lingtian Gao[a], T.X. Yu[b]

[a]*Department of Mechanics and Engineering Science, Peking University, Beijing 100871, PR China*
[b]*Department of Mechanical Engineering, Hong Kong University of Science & Technology, Clear Water Bay, Kowloon, Hong Kong*

Received 2 May 2003; received in revised form 22 August 2003; accepted 15 March 2004
Available online 28 October 2004

Abstract

In this investigation a characteristic analysis of stress wave propagation in anisotropic fluid-saturated porous media is performed based on generalized characteristic theory. This method enables us to carry out a complete basic analysis of wave propagation characteristic in fluid-saturated porous media, and immediately determine the wave fronts through the normal velocity surfaces. First, the characteristic differential equations and compatibility relations along bicharacteristics are deduced. Then the analytical expressions for the normal velocity surfaces and wave fronts are presented. Based on these equations, the characteristic of the normal velocity surfaces and the wave fronts for all components of the stress waves in an orthotropic fluid-saturated porous media as well as its special cases in three-dimensional space is computed and discussed. The results show that the wave fronts of fast and slow waves remain regular along with the increase of anisotropy of the media, but great anisotropy may lead to more than one triple angle on the wave fronts of quasi-transverse or transverse waves.

*Corresponding author. Current address: Institute of Mechanics, School of Civil Engineering, Beijing Jiaotong University, Beijing 100044, P.R. China.
E-mail address: y_liu@mail.china.com (Y. Liu).

0022-460X/$ - see front matter © 2004 Elsevier Ltd. All rights reserved.
doi:10.1016/j.jsv.2004.03.049

1. Introduction

The propagation of stress waves in anisotropic fluid-saturated porous media has important applications in many practical fields, such as geophysical exploration, earthquake engineering, rock dynamics, etc., owing to which it has attracted more and more attention in recent years. In 1956, Biot formulated the basic equations for the wave propagation in anisotropic porous media [1–4]. Based on his work, many researchers have studied the propagation characteristic of stress waves in fluid-saturated porous media using different methods. Plona [5] experimentally studied the slow wave predicted by Biot, and provided an experimental proof for Biot's theory. Auriault et al. [6] and Johnson [7] studied dynamic permeability. Tajuddin and Ahmed [8] calculated the dispersion curves for layered isotropic porous media. Schmitt [9] derived the characteristic equations for plane waves in transversely isotropic fluid-saturated porous media through homogenization theory and numerically discussed the dispersion and attenuation of different waves. Sharma and Gogna [10] also obtained the characteristic equations in rectangular coordinates and analyzed the characteristic of Rayleigh waves. Liu et al. [11–13] discussed the influence of anisotropy of solid skeleton and fluid viscosity on the propagation of stress waves. Carcione et al. [14] studied the velocity surface for a bone as an anisotropic fluid-saturated porous medium. It can be seen that the study for the wave characteristic in isotropic fluid-saturated porous media has approached the perfect characteristic. However, the theoretical analysis and numerical calculation of stress waves in anisotropic fluid-saturated porous media have not been carried out systematically, partly owing to the complexity of the media, and on the other hand, the scarcity of effective methods. Moreover, some basic characteristic of waves in anisotropic fluid-saturated porous media, such as the characteristic of velocity surfaces (or slowness surfaces) and wave fronts, plays a central role in the interpretation of a wide range of wave phenomena in anisotropic materials. Although some works have been carried out on the characteristic of velocity surfaces (or slowness surfaces) [14], to the author's knowledge, little attention has been paid to the research about the properties of the wave fronts. By now, how to accurately determine the wave fronts remains a key point for the characteristic analysis of stress wave propagation in anisotropic fluid-saturated porous media. Presently, we have had many methods to obtain the wave fronts, such as by drawing the enveloping surfaces after the slowness surfaces are determined [15], or through determining energy velocity surfaces by adopting plane-wave theory and introducing Umov–Poynting vector, which has been discussed in ref. [16]. However, for fluid-saturated porous media, the existence of the fluid phase will make the characteristic of velocity surfaces (or slowness surfaces) and wave fronts more complicated. It is necessary to find an explicit and simple method to discuss the basic characteristic of waves in anisotropic fluid-saturated porous media. The generalized characteristic theory and the method of characteristics are effective tools for the theoretical analysis and numerical calculation on the stress wave propagation problems. Different from the plane-wave theory, which should assume certain solution forms first, such as $u = u_0 \exp \mathrm{i}\,(kx - \omega t)$; the characteristic analysis solves the partial differential equations directly. As a result, in the plane-wave theory, the energy velocity (or the wave front) should be obtained in terms of Umov–Poynting vector and energy densities; while in characteristic analysis, the wave fronts could be immediately determined by the normal velocity surfaces and differential equations along bicharacteristics. Due to their extrusive advantage of explicit physical meaning, no discrete dispersion, high calculation efficiency and precision, the

characteristic analysis has been successfully and widely applied in the analysis for the propagation characteristic of stress waves in anisotropic solids [17]. However, little attention has been paid so far to the application of generalized characteristic theory in the analysis of stress wave propagation in anisotropic fluid-saturated porous media.

In this paper, a characteristic analysis for stress wave propagation in anisotropic fluid-saturated porous media is performed. The governing equations for anisotropic fluid-saturated porous media are obtained based on Biot's theory (Section 2). The characteristic differential equations and compatibility relations along bicharacteristics for anisotropic fluid-saturated porous media are deduced by using generalized characteristic theory (Section 3). The general analytical expressions for wave fronts and velocity surface are formulated. Moreover, three-dimensional velocity surfaces and wave fronts for all the components of the stress wave are completed with the help of our efforts on graphical interfaces and viewdata (Section 4). As a result, the features of stress wave propagation in orthotropic fluid-saturated porous media and its special cases, such as transversely isotropic fluid-saturated porous media and isotropic fluid-saturated porous media, are explored in detail (Section 5) and the conclusion is given.

2. Basic equations

2.1. Biot theory

For fluid-saturated porous medium, the equations of motion and the constitutive relation in Lagrange coordinate system may be expressed as [3]

$$\begin{aligned} \sigma_{ij,j} &= \rho_1 v^s_{i,t} + \rho_2 v^f_{i,t}, \\ -p_{,i} &= \rho_f v^s_{i,t} + \phi m_{ik}\,(v^f_{k,t} - v^s_{k,t}) + \phi r_{ik}\,(v^f_k - v^s_k), \end{aligned} \tag{1a}$$

$$\begin{aligned} \sigma_{ij,t} &= A_{ijkl}\, v^s_{k,l} + \phi M_{ij}(v^s_{k,k} - v^f_{k,k}), \\ p_{,t} &= M_{kl} v^s_{k,l} + \phi M\,(v^s_{k,k} - v^f_{k,k}), \end{aligned} \tag{1b}$$

where σ_{ij} are the stress components of solid skeleton, p the fluid pressure, ρ_ζ the density of ζ phase, in which $\zeta = s,f$, corresponding to the solid skeleton and pore fluid, respectively, $\rho = \rho_1 + \rho_2 = (1-\phi)\rho_s + \phi\rho_f$ denotes the solid–fluid mixture density, ϕ the porosity, and v^α_i the velocity components of ζ phase in the direction i. Repeated indices imply summation and the comma stands for partial derivative with respect to the space variable x_i or the time t. A_{ijkl}, M_{ij} and M are elastic parameters for anisotropic solid skeleton and the pore fluids. For orthotropic solid skeleton, the non-zero components of those can be written as [18]

$$\begin{aligned} &A_{11} = C_{11} + \alpha_1^2 M, \quad A_{12} = C_{12} + \alpha_1\alpha_2 M, \quad A_{13} = C_{13} + \alpha_1\alpha_3 M, \\ &A_{22} = C_{22} + \alpha_2^2 M, \quad A_{23} = C_{23} + \alpha_2\alpha_3 M, \quad A_{33} = C_{33} + \alpha_3^2 M, \\ &A_{44} = C_{44}, \quad A_{55} = C_{55}, \quad A_{66} = C_{66}, \\ &M_1 = -M\alpha_1, \quad M_2 = -M\alpha_2, \quad M_3 = -M\alpha_3, \end{aligned}$$

$$M = \left(\frac{1-\phi}{K_s} + \frac{\phi}{K_f} - \frac{C_{11}+C_{22}+C_{33}+2C_{12}+2C_{13}+2C_{23}}{9K_s^2} \right)^{-1},$$
$$\alpha_1 = 1 - \frac{C_{11}+C_{12}+C_{13}}{3K_s},\ \alpha_2 = 1 - \frac{C_{12}+C_{22}+C_{23}}{3K_s},\ \alpha_3 = 1 - \frac{C_{13}+C_{23}+C_{33}}{3K_s} \tag{2}$$

where C_{ij} are the elastic parameters for the solid skeleton, K_s the modulus of the solid grains, and K_f the modulus of the pore fluid. m_{ij} and r_{ij} are mass and damping symmetric matrixes. In order to compare with the results obtained in terms of the Umov–Poynting vector and energy densities, here m_{ij} and r_{ij} are expressed as the functions of angular frequency ω with the form

$$m_{ij}(\omega) = \mathrm{Re}[T_{ij}(\omega)]\rho_f/\phi,$$
$$r_{ij}(\omega) = \eta/\mathrm{Re}\,[K_{ij}(\omega)], \tag{3a}$$

where η is the viscosity of the fluid, and $K_{ij}(\omega)$ and $T_{ij}(\omega)$ are, respectively, dynamic permeability and tortuosity symmetric tensors with relation [7]

$$T_{ij}(\omega) = \mathrm{i}\eta\phi/[K_{ij}(\omega)\omega\rho_f] \tag{3b}$$

in which i denotes the imaginary unit. In this paper, without special declaration, $i,j = 1,2,3$ correspond to x, y, z, respectively.

2.2. Dynamic permeability and tortuosity

For porous solids with pores of simple form (for example, cylinder tubes), the dynamic permeability and dynamic tortuosity can be expressed in closed form [6,7]. For orthotropic fluid-saturated porous media, by assuming that the main symmetric axis of orthotropic solid skeleton and the complex permeability tensor are both along the vertical direction, the dynamic permeability tensor is expressed as

$$[K_{ij}(\omega)] = \begin{bmatrix} k_1(\omega) & 0 & 0 \\ 0 & k_2(\omega) & 0 \\ 0 & 0 & k_3(\omega) \end{bmatrix}, \tag{4}$$

where $k_1(\omega), k_2(\omega)$ and $k_3(\omega)$ are dynamic permeabilities along the orthotropic main axes (i.e., axes x, y and z). Extending the formula given by Ref. [7] to the orthotropic situation, we obtain

$$k_j(\omega) = k_{j0}\left[\left(1 - \frac{4\mathrm{i}T_{j\infty}^2 k_{j0}^2 \omega\rho_f}{\eta\Lambda_j^2\phi^2} \right)^{0.5} - \frac{\mathrm{i}T_{j\infty}k_{j0}\omega\rho_f}{\eta\phi} \right]^{-1}, \tag{5}$$

where Λ_j is the characteristic length of pores in the j direction, $T_{j\infty}$ the dynamic tortuosity when ω tends to infinity, k_{j0} the dynamic permeability when ω equals zero. The dynamic tortuosity T_j may be obtained by Eq. (3b). $T_{j\infty}$, k_{j0} and Λ_j are unrelated and independently measured [7]. Eq. (5) merely relies on four constants $T_{j\infty}$, k_{j0}, Λ_j and ϕ, which are easy to be determined, and are

applicable in the whole real frequency domain. In the following calculation, we have [7]

$$\frac{8T_{j\infty}k_{j0}}{\phi\Lambda_j^2} = 1. \tag{6}$$

3. Characteristic form

Let the characteristic surface in the $(\mathbf{x}, t)$ space be given by

$$\psi = t - \tau(\mathbf{x}) = 0, \tag{7}$$

where τ is a function of $\mathbf{x}$ only, $\mathbf{x} = \{x, y, z\}$. Also, let $\tilde{f}$ be the value of function $f(\mathbf{x}, t)$ evaluated on the characteristic surface $t = \tau(\mathbf{x})$, i.e.,

$$\tilde{f}(\mathbf{x}, t) = f(\mathbf{x}, \tau(\mathbf{x})). \tag{8}$$

We then have

$$\tilde{f}_{,i} = f_{,i} + f_{,t}\tau_{,i}, \tag{9}$$

where $f_{,i}$ and $f_{,t}$ on the right-hand side of Eq. (9) are the values of the partial differentiations of function f with respect to the spacial variables and time, respectively, evaluated on the characteristic surface. By applying Eq. (9) to σ_{ij} and p in Eq. (1), we obtain

$$\begin{aligned} \tilde{\sigma}_{ij,j} - \sigma_{ij,\,t}\tau_{,\,j} &= \rho_1 v^s_{i,t} + \rho_2\, v^f_{i,t} \\ -\tilde{p}_{,i} + p_{,t}\tau_{,i} &= \rho_f v^s_{i,t} + \phi m_{ik}(v^f_{k,t} - v^s_{k,t}) + \phi r_{ik}(v^f_k - v^s_k), \end{aligned} \tag{10a}$$

$$\begin{aligned} \sigma_{ij,t} &= A_{ijkl}(\tilde{v}^s_{k,l} - v^s_{k,t}\tau_{,l}) + \phi M_{ij}(\tilde{v}^s_{k,k} - v^s_{k,t}\tau_{,k} - \tilde{v}^f_{k,k} + v^f_{k,t}\tau_{,k}), \\ p_{,t} &= M_{kl}(\tilde{v}^s_{k,l} - v^s_{k,t}\tau_{,l}) + \phi M(\tilde{v}^s_{k,k} - v^s_{k,t}\tau_{,k} - \tilde{v}^f_{k,k} + v^f_{k,t}\tau_{,k}), \end{aligned} \tag{10b}$$

After eliminating $\sigma_{ij,t}$ and $p_{,t}$, we have

$$\begin{bmatrix} D^*_{ik} & M^*_{ik} \\ \bar{M}^*_{ik} - M^o_{ik} & M^o_{ik} \end{bmatrix} \begin{Bmatrix} v^s_{k,t} \\ v^f_{k,t} \end{Bmatrix} = \begin{Bmatrix} A^1_i \\ A^2_i \end{Bmatrix}, \tag{11}$$

where

$$D^*_{ik} = A_{ijkl}\tau_{,j}\,\tau_{,l} + \phi M_{ij}\tau_{,j}\tau_{,k} - \rho_1\delta_{ik}, \tag{12a}$$

$$M^*_{ik} = -\phi M_{ij}\tau_{,j}\,\tau_{,k} - \rho_2\delta_{ik}, \tag{12b}$$

$$\bar{M}^*_{ik} = -M_{kl}\tau_{,i}\tau_{,l} - \rho_f\delta_{ik}, \tag{12c}$$

$$M^o_{ik} = \phi M\tau_{,i}\tau_{,k} - \phi m_{ik}, \tag{12d}$$

$$A^1_i = A_{ijkl}\tilde{v}^s_{k,l}\tau_{,j} + \phi M_{ij}\tilde{v}^s_{k,k}\tau_{,j} - \phi M_{ij}\tilde{v}^f_{k,k}\tau_{,j} - \tilde{\sigma}_{ij,j}, \tag{12e}$$

$$A^2_i = -M_{kl}\tilde{v}^s_{k,l}\tau_{,i} + \phi M\tilde{v}^f_{k,k}\,\tau_{,i} - \phi M\,\tilde{v}^s_{k,k}\tau_{,i} + \tilde{p}_{,i} + \phi r_{ik}(v^f_k - v^s_k). \tag{12f}$$

The characteristic surface $\tau(\mathbf{x})$ is a solution of the differential equations which is obtained by setting the determinant of the matrix as zero, that is,

$$|Q_{ik}| = \begin{vmatrix} D^*_{ik} & M^*_{ik} \\ \bar{M}^*_{ik} - M^o_{ik} & M^o_{ik} \end{vmatrix} = 0. \tag{13}$$

At a fixed time t, let $\mathbf{n}$ be the unit vector normal to the characteristic surface in the $\mathbf{x}$-space pointing toward the direction of propagation of the characteristic surface and c be the normal wave speed. Then

$$\tau_{,i} = n_i/c. \tag{14}$$

Substituting Eq. (14) into Eq. (12) and then into Eq. (13) yields the characteristic equations for wave speeds c along a given vector $\mathbf{n}$.

Since the characteristic curves of Eq. (13) are the bicharacteristics of Eq. (1), we obtain [17]

$$b_p = \frac{\mathrm{d}x_p}{\mathrm{d}t} = \frac{(\partial\mathbf{Q}/\partial\tau_{,p})}{\tau_{,k}(\partial\mathbf{Q}/\partial\tau_{,k})} \quad (p = 1, 2, 3), \tag{15}$$

where b_p is the wave velocity measured along the bicharacteristic direction.

For every value of b_p, we can find the corresponding left eigenvectors $\mathbf{l} = \{\mathbf{l}^1, \mathbf{l}^2\}$ of $\mathbf{Q}$, that is

$$\mathbf{l}^1\mathbf{D} + \mathbf{l}^2(\mathbf{M}^* - \mathbf{M}^o) = 0, \tag{16a}$$

$$\mathbf{l}^1\mathbf{M}^* + \mathbf{l}^2\mathbf{M}^o = 0 \tag{16b}$$

in which $\mathbf{l}^1 = \{l^1_1, l^1_2, l^1_3\}, \mathbf{l}^2 = \{l^2_1, l^2_2, l^2_3\}$. When Eq. (11) is multiplied by $\mathbf{l}$, it is found from Eqs. (16) that

$$\mathbf{l}^1\mathbf{A}^1 + \mathbf{l}^2\mathbf{A}^2 = 0. \tag{17}$$

Because $\tilde{\sigma}_{ij}$, $\tilde{v}^\zeta_k$ and $\tilde{p}$ are the values of σ_{ij}, v^ζ_k and p evaluated on the characteristic surface, Eq. (17) is just the 'interior differential equation' on the characteristic surface.

The total differentiation of a function $f(\mathbf{x}, t)$ along the bicharacteristics is defined by

$$\frac{\mathrm{d}f}{\mathrm{d}t} = f_{,j}\frac{\mathrm{d}x_j}{\mathrm{d}t} + f_{,t} = f_{,j}\, b_{,j} + f_{,t}. \tag{18}$$

Eliminating $f_{,t}$ from Eqs. (9) and (18) yields

$$\tilde{f}_{,i} = \frac{\mathrm{d}f}{\mathrm{d}t}\tau_{,i} + (\delta_{ij} - \tau_{,i}b_{,j})f_{,j}. \tag{19}$$

Therefore, using Eqs. (19), (14) and (16), Eq. (17) can be rewritten as

$$l^1_i\left(\frac{\mathrm{d}\sigma_{ij}}{\mathrm{d}t}n_j - \rho_1 c\frac{\mathrm{d}v^s_i}{\mathrm{d}t} - \rho_2 c\frac{\mathrm{d}v^f_i}{\mathrm{d}t}\right) - l^2_i\left[\frac{\mathrm{d}p}{\mathrm{d}t}n_i + \rho_f c\frac{\mathrm{d}v^s_i}{\mathrm{d}t} - \phi c m_{ik}\frac{\mathrm{d}v^s_k}{\mathrm{d}t} + \phi c m_{ik}\frac{\mathrm{d}v^f_k}{\mathrm{d}t}\right] = S \quad \text{along } \frac{\mathrm{d}x_i}{\mathrm{d}t} = b_i, \tag{20a}$$

where

$$S = \Big[l_i^1 \left(A_{ilkl} n_j + \phi M_{ik} n_j - \rho_1 c \delta_{ik} b_j \right) - l_i^2 \Big(M_{kj}\, n_i + \phi M \delta_{kj} n_i - \phi m_{ik} b_j + \rho_f c \delta_{ik} b_j \Big) \Big] v_{k,j}^s + \left[l_i^1 (-\phi M_{ik}\, n_j - \rho_2 c \delta_{ik} b_j) + l_i^2 (\phi M \delta_{jk} n_i - \phi\, m_{ik} b_j) \right] v_{k,j}^f - l_i^1 (c\delta_{jk} - n_j b_k)\sigma_{ij,k} + l_i^2 (c\delta_{ik} - n_i b_k) p_{,k} + l_i^2 \phi c r_{ik} (v_k^f - v_k^s). \tag{20b}$$

The interior differentiation on the characteristic surface in the space (x, t) is now divided into two parts. The left-hand side of Eq. (20a) contains differentiations along the bicharacteristics, while the right-hand side contains differentiations on the part of characteristic surface, which intersects the plane $t = \text{const}$. Eqs. (20) are the desired compatibility relations along bicharacteristics, which provides a basis for a finite-difference approximation.

The above analysis results can be easily applied to zero-porosity porous media. The constitutive equations for anisotropic solids can be obtained from Eqs. (1) by setting $\phi = 0$, $\rho_f = 0$, $A_{ijkl} = C_{ijkl}$, $\rho_1 = \rho_s$, $m_{ij} = r_{ij} = 0$, and $M_{ij} = M = 0$. The differential equations for anisotropic solids are obtained through direct degeneration of Eq. (11)

$$D'^{*}_{ik} v^s_{k,t} = A'_i, \tag{21}$$

where

$$D'^{*}_{ik} = C_{ijkl} \tau_{,j} \tau_{,l} - \rho_s \delta_{ik}. \tag{22a}$$

$$A'_i = C_{ijkl} \tilde{v}^s_{k,l} \tau_{,j} - \tilde{\sigma}_{ij,j} \tag{22b}$$

Thus, the differentiation equation of the characteristic surface for anisotropic solids is determined by

$$\left| D'^{*}_{ik} \right| = \left| C_{ijkl} \tau_{,j} \tau_{,l} - \rho_s \delta_{ik} \right| = 0. \tag{23}$$

Accordingly, the compatibility relations along bicharacteristics are

$$l_i \left(\frac{\mathrm{d}\sigma_{ij}}{\mathrm{d}t} n_j - \rho_s c \frac{\mathrm{d}v_i^s}{\mathrm{d}t} \right) = S' \quad \text{along } \frac{\mathrm{d}x_i}{\mathrm{d}t} = b_i, \tag{24a}$$

where

$$S' = l_i (C_{ijkl} n_j - \rho_s c \delta_{ik} b_l)\, v^s_{k,l} - l_i (c\delta_{kj} - n_j b_k)\sigma_{ij,k} \tag{24b}$$

and l_i represents the corresponding left vector of characteristic matrix $\mathbf{D}'^{*}$. Hence, the characteristic equations and compatibility relations for anisotropic solids, obtained through the degeneration of the equations for anisotropic fluid-saturated porous media, coincide with the formula given in Ref. [15]. This indicates that the characteristic equations for pure solids form a particular case of fluid-saturated porous media and can be degenerated directly from the corresponding characteristic equations for fluid-saturated porous media.

4. Wave fronts and velocity surfaces

4.1. Wave fronts

Assume a disturbance is applied at the origin O at $t=0$. If t is the arrival time, the first plane wave $n(\mathbf{x})$ to arrive at the point $\mathbf{r}$ must satisfy [19]

$$\mathbf{r}\bullet\mathbf{n}(\mathbf{x}) = v(\mathbf{x})\, t. \tag{25}$$

Following Ref. [19], for a given time (say $t=1$) the wave surface is defined as the locus of point $\mathbf{r}$, which satisfies

$$\mathbf{r}\bullet\mathbf{s} = 1, \tag{26}$$

where vector $\mathbf{s}$ is the slowness vector defined by

$$\mathbf{s} = \frac{\mathbf{n}(\mathbf{x})}{v(\mathbf{x})} \tag{27}$$

and the surface $1/v(\mathbf{x})$ is the slowness surface. Eqs. (26) and (27) show that instead of finding $\mathbf{n}(\mathbf{x})$ for a given $\mathbf{r}$, we could determine $\mathbf{r}$ for a given n such that Eq. (26) is satisfied.

From Eq. (14), it is easy to know that the projections of the coordinates of points on slowness surface to the axis x_i are

$$s_i = \frac{1}{c} n_i = \tau_{,i}, \tag{28}$$

where $\tau_{,i}$ is the solution of the characteristic Eq. (13). Eq. (13) can be expressed as

$$F(\tau_{,i}) = 0. \tag{29}$$

By treating Eq. (29) as the first-order differential equation of τ, then the differential equations along bicharacteristics are

$$\frac{\mathrm{d}x_i}{\mathrm{d}s} = \frac{\partial F}{\partial \tau_{,i}}, \tag{30a}$$

$$\frac{\mathrm{d}\tau}{\mathrm{d}s} = \tau_{,i}\frac{\partial F}{\partial \tau_{,i}}, \tag{30b}$$

$$\frac{\mathrm{d}\tau_{,i}}{\mathrm{d}s} = -\left(\tau_{,i}\frac{\partial F}{\partial \tau} + \frac{\partial F}{\partial x_i}\right), \tag{30c}$$

where the direction of $\partial F/\partial\tau_{,i}$ is parallel to the direction of vector $\mathbf{s}$. From Eq. (26) it is easy to see that the direction of $\partial F/\partial\tau_{,i}$ is just the direction of vector $\mathbf{r}$. Then, what should be determined by now is the module of vector $\mathbf{r}$. Along the bicharacteristics, $t=\tau(\tilde{x})$, and we have

$$\frac{\mathrm{d}x_i}{\mathrm{d}t} = \frac{\mathrm{d}x_i}{\mathrm{d}\tau} = \frac{\mathrm{d}x_i}{\mathrm{d}s} \Big/ \frac{\mathrm{d}\tau}{\mathrm{d}s}. \tag{31}$$

Suppose that r is the module of vector $\mathbf{r}$, and r_i is the projection of $\mathbf{r}$ on the axes, then when $t=1$,

we have

$$\frac{\mathrm{d}x_i}{\mathrm{d}t} = r_i. \tag{32}$$

Substituting Eqs. (30a) and (30b) into Eq. (32) leads to

$$r_i = \frac{\partial F}{\partial \tau_{,i}} / (\tau_{,j} \frac{\partial F}{\partial \tau_{,j}}). \tag{33}$$

By now, we have obtained the expressions for the coordinates of the points on the wave fronts, that is, the expressions for wave fronts.

4.2. Normal velocity surfaces

Here we deduce the expressions for the normal velocity surfaces of orthotropic fluid-saturated porous media. By using Eq. (2), Eq. (11) is recast as

$$\mathbf{D}^* \mathbf{V}_{,t} = \mathbf{A}, \tag{34}$$

where

$$\mathbf{V}_{,t} = \{v^s_{x,t}, v^s_{y,t}, v^s_{z,t}, v^f_{x,t}, v^f_{y,t}, v^f_{z,t}\}^{\mathrm{T}},$$

the elements for matrix $\mathbf{D}^*$and $\mathbf{A}$ are

$$\begin{aligned}
&d^*_{11} = A_{11}\tau^2_{,x} + A_{66}\tau^2_{,y} + A_{55}\tau^2_{,z} + \phi M_1 \tau^2_{,x} - \rho_1, \quad d^*_{12} = A_{12}\,\tau_{,x}\tau_{,y} + A_{66}\tau_{,x}\tau_{,y} + \phi M_1 \tau_{,x}\tau_{,y},\\
&d^*_{13} = A_{13}\tau_{,x}\tau_{,z} + A_{55}\tau_{,x}\tau_{,z} + \phi M_1 \tau_{,x}\tau_{,z}, \quad d^*_{14} = -\phi M_1 \tau^2_{,x} - \rho_2,\\
&d^*_{15} = -\phi M_1 \tau_{,x}\tau_{,y}, \quad d^*_{16} = -\phi M_1 \tau_{,x}\tau_{,z},\\
&d^*_{21} = A_{12}\tau_{,x}\tau_{,y} + A_{66}\tau_{,x}\tau_{,y} + \phi M_2 \tau_{,x}\tau_{,y}, \quad d^*_{22} = A_{66}\tau^2_{,x} + A_{22}\tau^2_{,y} + A_{44}\tau^2_{,z} + \phi M_2 \tau^2_{,y} - \rho_1,\\
&d^*_{23} = A_{23}\tau_{,y}\tau_{,z} + A_{44}\tau_{,y}\tau_{,z} + \phi M_2 \tau_{,y}\tau_{,z}, \quad d^*_{24} = -\phi M_2 \tau_{,x}\tau_{,y},\\
&d^*_{25} = -\phi M_2 \tau^2_{,y} - \rho_2, \quad d^*_{26} = -\phi M_2 \tau_{,y}\tau_{,z},\\
&d^*_{31} = A_{13}\tau_{,x}\tau_{,z} + A_{55}\tau_{,x}\tau_{,z} + \phi M_3 \tau_{,x}\tau_{,z}, \quad d^*_{32} = A_{23}\tau_{,y}\tau_{,z} + A_{44}\tau_{,y}\tau_{,z} + \phi M_3 \tau_{,y}\tau_{,z},\\
&d^*_{33} = A_{55}\tau^2_{,x} + A_{44}\tau^2_{,y} + A_{33}\tau^2_{,z} + \phi M_3 \tau^2_{,z} - \rho_1, \quad d^*_{34} = -\phi M_3 \tau_{,x}\tau_{,z},\\
&d^*_{35} = -\phi M_3 \tau_{,y}\tau_{,z}, \quad d^*_{36} = -\phi M_3 \tau^2_{,z} - \rho_2,\\
&d^*_{41} = \phi m_1 - \rho_f - M_1 \tau^2_{,x} - \phi M \tau^2_{,x}, \quad d^*_{42} = -M_2 \tau_{,x}\tau_{,y} - \phi M \tau_{,x}\tau_{,y},\\
&d^*_{43} = -\phi M \tau_{,x}\tau_{,z} - M_3 \tau_{,x}\tau_{,z}, \quad d^*_{44} = -\phi m_1 + \phi M \tau^2_{,x},\\
&d^*_{45} = \phi M \tau_{,x}\tau_{,y}, \quad d^*_{46} = \phi M \tau_{,x}\tau_{,z},\\
&d^*_{51} = -M_1 \tau_{,x}\tau_{,y} - \phi M \tau_{,x}\tau_{,y}, \quad d^*_{52} = \phi m_2 - \rho_f - M_2 \tau^2_{,y} - \phi M \tau^2_{,y},
\end{aligned}$$

$$
\begin{aligned}
d^*_{53} &= -\phi M\tau_{,y}\tau_{,z} - M_3\tau_{,y}\tau_{,z}, \quad d^*_{54} = \phi M\tau_{,x}\tau_{,y},\\
d^*_{55} &= -\phi m_2 + \phi M\tau^2_{,y}, \quad d^*_{56} = \phi M\tau_{,y}\tau_{,z},\\
d^*_{61} &= -M_1\tau_{,x}\tau_{,z} - \phi M\tau_{,x}\tau_{,z}, \quad d^*_{62} = -M_2\tau_{,y}\tau_{,z} - \phi M\tau_{,y}\tau_{,z},\\
d^*_{63} &= \phi m_3 - \rho_f - M_3\tau^2_{,z} - \phi M\tau^2_{,z}, \quad d^*_{64} = \phi M\tau_{,x}\tau_{,z},\\
d^*_{65} &= \phi M\tau_{,y}\tau_{,z}, \quad d^*_{66} = -\phi m_3 + \phi M\tau^2_{,z},
\end{aligned} \tag{35a}
$$

$$
\begin{aligned}
A_1 = {} & -\tilde{\sigma}_{xx,x} - \tilde{\sigma}_{xy,y} - \tilde{\sigma}_{xz,z} + A_{66}\tau_{,y}(\tilde{v}^s_{x,y} + \tilde{v}^s_{y,x}) + A_{55}\tau_{,z}(\tilde{v}^s_{x,z} + \tilde{v}^s_{z,x})\\
& + \tau_{,x}(A_{11}\tilde{v}^s_{x,x} + A_{12}\tilde{v}^s_{y,y} + A_{13}\tilde{v}^s_{z,z})\\
& - \phi M_1\tau_{,x}(\tilde{v}^f_{x,x} + \tilde{v}^f_{y,y} + \tilde{v}^f_{z,z} - \tilde{v}^s_{x,x} - \tilde{v}^s_{y,y} - \tilde{v}^s_{z,z}),\\
A_2 = {} & -\tilde{\sigma}_{x,y,x} - \tilde{\sigma}_{yy,y} - \tilde{\sigma}_{yz,z} + A_{66}\tau_{,x}(\tilde{v}^s_{x,y} + \tilde{v}^s_{y,x})\\
& + A_{44}\tau_{,z}(\tilde{v}^s_{y,z} + \tilde{v}^s_{z,y}) + \tau_{,y}(A_{12}\tilde{v}^s_{x,x} + A_{22}\tilde{v}^s_{y,y} + A_{23}\tilde{v}^s_{z,z})\\
& - \phi M_2\tau_{,y}(\tilde{v}^f_{x,x} + \tilde{v}^f_{y,y} + \tilde{v}^f_{z,z} - \tilde{v}^s_{x,x} - \tilde{v}^s_{y,y} - \tilde{v}^s_{z,z}),\\
A_3 = {} & -\tilde{\sigma}_{xz,x} - \tilde{\sigma}_{yz,y} - \tilde{\sigma}_{zz,z} + A_{55}\tau_{,x}(\tilde{v}^s_{x,z} + \tilde{v}^s_{z,x})\\
& + A_{44}\tau_{,y}(\tilde{v}^s_{y,z} + \tilde{v}^s_{z,y}) + \tau_{,z}(A_{13}\tilde{v}^s_{x,x} + A_{23}\tilde{v}^s_{y,y} + A_{33}\tilde{v}^s_{z,z})\\
& - \phi M_3\tau_{,z}(\tilde{v}^f_{x,x} + \tilde{v}^f_{y,y} + \tilde{v}^f_{z,z} - \tilde{v}^s_{x,x} - \tilde{v}^s_{y,y} - \tilde{v}^s_{z,z}),\\
A_4 = {} & \tilde{p}_{,x} + \phi M\tau_{,x}(\tilde{v}^f_{x,x} + \tilde{v}^f_{y,y} + \tilde{v}^f_{z,z})\\
& - \phi M\tau_{,x}(\tilde{v}^s_{x,x} + \tilde{v}^s_{y,y} + \tilde{v}^s_{z,z})\\
& - \tau_{,x}(M_1\tilde{v}^s_{x,x} + M_2\tilde{v}^s_{y,y} + M_3\tilde{v}^s_{z,z}) + \phi r_1(v^f_z - v^s_z),\\
A_5 = {} & \tilde{p}_{,y} + \phi M\tau_{,y}(\tilde{v}^f_{x,x} + \tilde{v}^f_{y,y} + \tilde{v}^f_{z,z})\\
& - \phi M\tau_{,y}(\tilde{v}^s_{x,x} + \tilde{v}^s_{y,y} + \tilde{v}^s_{z,z})\\
& - \tau_{,y}(M_1\tilde{v}^s_{x,x} + M_2\tilde{v}^s_{y,y} + M_3\tilde{v}^s_{z,z}) + \phi r_2(v^f_y - v^s_y),\\
A_6 = {} & \tilde{p}_{,z} + \phi M\tau_{,z}(\tilde{v}^f_{x,x} + \tilde{v}^f_{y,y} + \tilde{v}^f_{z,z})\\
& - \phi M\tau_{,z}(\tilde{v}^s_{x,x} + \tilde{v}^s_{y,y} + \tilde{v}^s_{z,z})\\
& - \tau_{,z}(M_1\tilde{v}^s_{x,x} + M_2\tilde{v}^s_{y,y} + M_3\tilde{v}^s_{z,z}) + \phi r_3(v^f_z - v^s_z).
\end{aligned} \tag{35b}
$$

Thus, the differential equation of the characteristic surface is determined by

$$\text{Det}\,\mathbf{D}^* = 0. \tag{36}$$

Let $\mathbf{n} = (\cos\,\alpha, \cos\,\beta,\, \cos\gamma)$ be the unit vector normal to the characteristic surface, in which α, β and γ are the angles between the vector n and axis x axis y and axis z, respectively. Then we have

$$\tau_{,x} = \frac{\cos\,\alpha}{c}\ \tau_{,y} = \frac{\cos\,\beta}{c}\ \tau_{,z} = \frac{\cos\,\gamma}{c}. \tag{37}$$

Substituting Eqs. (37) into Eq. (36), we obtained the characteristic equations for the normal velocity surface, that is

$$|\mathbf{D}_v| = 0. \tag{38}$$

The elements of $\mathbf{D}_v$ have the same forms as the elements given in Eqs. (35a), except that $\tau_{,i}$ is replaced by the relations listed in Eqs. (37). Expanding Eq. (38) leads to

$$a_1c^8 + a_2c^6 + a_3c^4 + a_4c^2 + a_5 = 0. \tag{39}$$

The explicit forms of the coefficients a_m ($m = 1,\ldots,5$) are very miscellaneous, so they are not given here. Eq. (39) is quartic of c^2which can be solved directly. Thus, for a given vector $\mathbf{n}$, four positive velocities—the velocity for quasi-fast wave, marked as 'qL1', quasi-slow wave, marked as 'qL2', and quasi-transverse waves, marked as 'qS1' and 'qS2', are obtained.

4.3. Special cases

The above expressions for wave fronts and velocity surfaces can be easily applied to the cases of transversely isotropic fluid-saturated porous media, isotropic fluid-saturated porous media, orthotropic solids (also refer to Section 3), transversely isotropic solids and isotropic solids. For example, in the case of isotropic fluid-saturated porous media, by setting $C_{11} = C_{22} = C_{33}$, $C_{12} = C_{13} = C_{23}$, $C_{44} = C_{55} = C_{66}$ and $2C_{44} = C_{11} = C_{12}$, and without loss of generality let $\mathbf{n} = (1,0,0)$; Eq. (39) is degenerated to

$$\begin{aligned}&[(\rho m_1 - \rho_f^2)c^2 - A_{66}m_1]\,[(\rho m_1 - \rho_f^2)c^4 - (\rho M + A_{11}m_1 + 2M_1\rho_f)c^2\\ &+ A_{11}M - M_1^2] = 0.\end{aligned} \tag{40}$$

The velocities for the waves are

$$c_s^2 = \frac{A_{44}m_1}{\rho m_1 - \rho_f^2}, \tag{41a}$$

$$c_{L1}^2 = \frac{\Delta + \sqrt{\Delta^2 - 4(\rho m_1 - \rho_f^2)(A_{11}M - M_1^2)}}{2(\rho m_1 - \rho_f^2)}, \tag{41b}$$

$$c_{L2}^2 = \frac{\Delta - \sqrt{\Delta^2 - 4(\rho m_1 - \rho_f^2)(A_{11}M - M_1^2)}}{2(\rho m_1 - \rho_f^2)}, \tag{41c}$$

where $\Delta = \rho M + A_{11}m_1 + 2M_1\rho_f$.

For isotropic solids, the expressions of wave velocity can be obtained from Eq. (39) after the same degeneration as Eq. (21), that is,

$$c_s^2 = \frac{C_{44}}{\rho}, \tag{42a}$$

$$c_L^2 = \frac{C_{11}}{\rho}. \tag{42b}$$

They are the familiar formulae for velocities of the transverse wave and longitudinal wave in isotropic solids.

5. Numerical results and discussion

The shape of normal velocity surfaces (or slowness surfaces, which are the inverse of velocity surfaces) and wave fronts is important in the interpretation of wave phenomena and nowadays it forms the basic concept underlying the treatment of diverse problems such as the propagation of surface waves, elastodynamic Green's functions and phonon focusing in ballistic phonon transport [20]. In order to generalize the features of stress wave propagation in fluid-saturated porous media, several numerical examples are computed so as to obtain normal velocity surfaces and wave fronts for an orthotropic fluid-saturated porous medium and its special cases according to the equations derived above. The parameters for the orthotropic fluid-saturated porous medium are given in Table 1. In all calculations, the frequency takes the value of 3135 Hz, which is the same as that in Ref. [16].

Figs. 1 and 2 show the three-dimensional normal velocity surfaces and wave fronts for stress wave propagation in the orthotropic fluid-saturated porous medium. Due to the symmetry, only parts of the first quadrant are given. From Figs. 1 and 2, it can be seen that there are four kinds of waves: quasi-fast wave, marked as 'qL1'; quasi-slow wave, marked as 'qL2'; and quasi-transverse waves, marked as 'qS1' and 'qS2', respectively. The wave qL2 is a particular wave for fluid-saturated porous media which mainly accounts for the effect of the fluid. In Fig. 1, V_x, V_y and V_z mean the projections of the speed c, obtained through Eq. (38), on the axis x, y and z, respectively. As shown in Figs. 1 and 2, the velocity surfaces and wave fronts are complex three-dimensional surfaces. In order to demonstrate this irregularity in a conventional way, the projections of the velocity surfaces and wave fronts on the plane xOy, xOz, and yOz are also plotted in Figs. 3–5.

Shown as Figs. 1 and 2, due to anisotropy of the media, the velocity surfaces and the wave fronts change with the propagation direction of the stress waves. The velocity surfaces for qL1 and qL2 are relatively regular and convex, as shown in Figs. 1a and b. But the velocity surfaces for qS1 and qS2 are very anisotropic and display concave and saddle-shaped regions in addition to convex regions, which are given in Figs. 1c and d. As a result, the wave fronts for qL1 and qL2 are anisotropic simple surfaces, and the wave fronts for qS1 and qS2 exhibit complex characteristic and there are more than one cuspidal triple angle on them. The three-dimensional variation of the wave fronts for qS1 and qS2 are given in Figs. 2c and d. By referring to Figs. 3b, 4b and 5b, the projections of the wave fronts on the plane xOy, xOz, and yOz, it can be seen clearly that there are three triple angles on the wave front of qS1 and one on the wave front of qS2. The positions and sizes of the triple angles show directional dependence. For example, there are two triple angles in the plane xOz, but only one in the plane yOz for qS1. This variation of the numbers, position and

Table 1
Parameters for orthotropic fluid-saturated porous media (porosity $\phi = 0.2$)

$C_{11} = 39.4$ GPa	$C_{33} = 13.1$ GPa	$k_{20} = 400$ mD	$K_s = 40$ GPa
$C_{12} = 1.0$ GPa	$C_{44} = 3.0$ GPa	$k_{30} = 100$ mD	$K_f = 2.5$ GPa
$C_{13} = 5.38$ GPa	$C_{55} = 16.0$ GPa	$T_1 = 2$ mD	$\rho_f = 1040$ kg/m^2
$C_{22} = 38.0$ GPa	$C_{66} = 18.0$ GPa	$T_2 = 3.0$ mD	$\rho_s = 1815$ kg/m^2
$C_{23} = 4.0$ GPa	$k_{10} = 600$ mD	$T_3 = 3.6$ mD	$\eta = 0.001$ Pa s

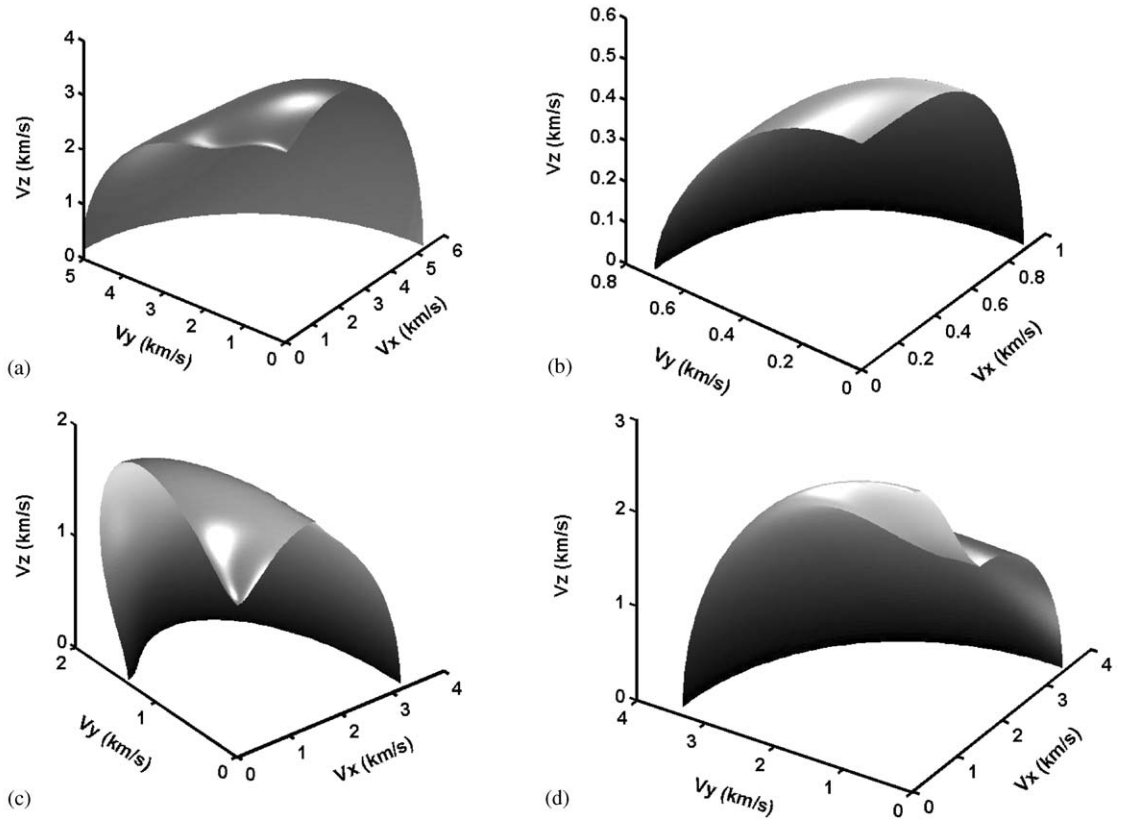

Fig. 1. (a) Velocity surface of qL1 in the first quadrant for orthotrophic fluid-saturated porous media. (b) Velocity surface of qL2 in the first quadrant for orthotropic fluid-saturated porous media. (c) Velocity surface of qS1 in the first quadrant for orthotrophic fluid-saturated porous media. (d) Velocity surface of qS2 in the first quadrant for orthotropic fluid-saturated porous media.

sizes of triple angles from plane xOz to yOz is shown clearly in Fig. 2c. Those further reflect the complicated influence of anisotropy of media on the propagation characteristic of stress waves.

Subsequently, we let $C_{11}=C_{22}=39.4\,\text{GPa}$, $C_{13}=C_{23}=5.38\,\text{GPa}$, $C_{44}=C_{55}=3\,\text{GPa}$, $C_{66}=(C_{11}-C_{12})/2=19.2\,\text{GPa}$, $k_1=k_2=600\,\text{mD}$, $T_1=T_2\,\text{mD}$ (referring to Table 1), and discuss the wave propagation in the transversely isotropic fluid-saturated porous medium. The calculating parameters are the same with those given in Ref. [16].

Figs. 6 and 7 describe the velocity surfaces and wave fronts in iso–plane xOy and aniso–plane xOz for the transversely isotropic fluid-saturated porous medium, respectively. Comparison between Fig. 6 and Fig. 3 shows that in iso-plane of the transversely isotropic fluid-saturated porous medium, the velocity surfaces and wave fronts are circles and coincide with each other. However, in aniso-plane xOz, as shown in Fig. 7, velocity surfaces and wave fronts show direction dependence. But the numbers of triple angles on the wave fronts for the transversely

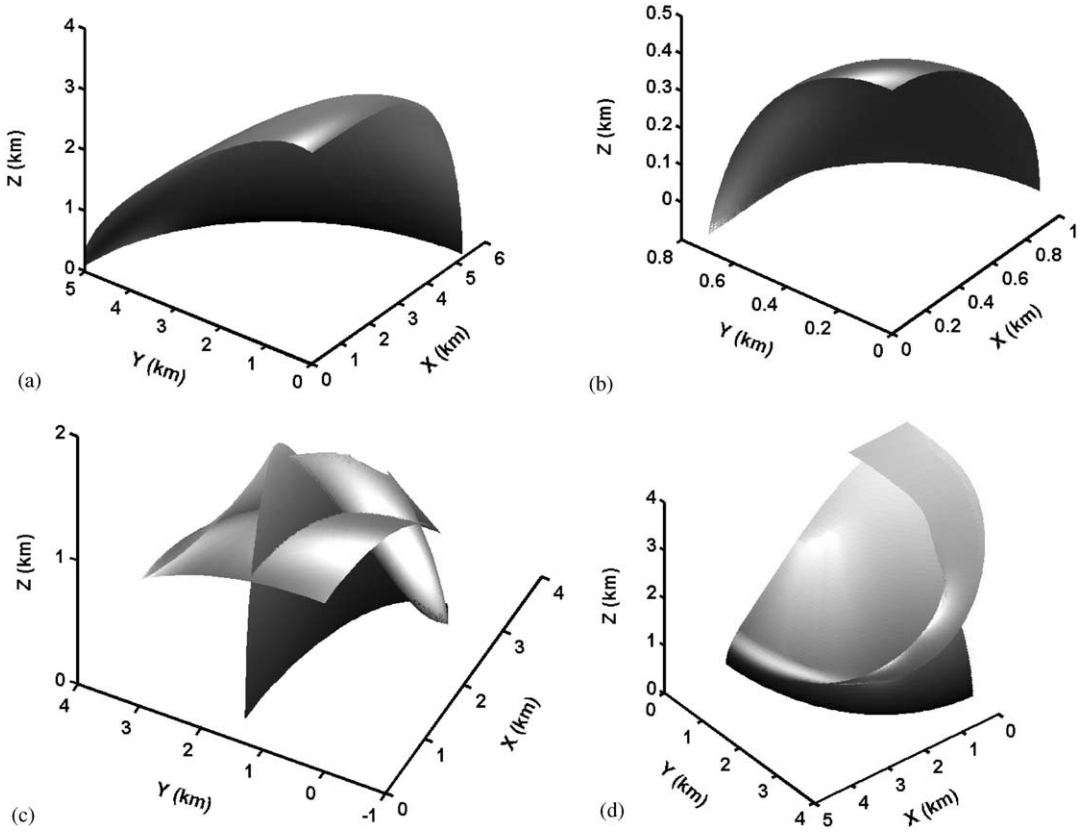

Fig. 2. (a) Wave fronts of qL1 in the first quadrant for orthotropic fluid-saturated porous media. (b) Wave fronts of qL2 in the first quadrant for orthotropic fluid-saturated porous media. (c) Wave fronts of qS1 in the first quadrant for orthotropic fluid-saturated porous media. (d) Wave fronts of qS2 in the first quadrant for orthotropic fluid-saturated porous media.

isotropic fluid-saturated porous medium are less than those for orthotropic medium and the shapes seem simpler, compared with Fig. 4. This is owing to the less severe anisotropy of the medium. Comparing Figs. 6a and b with Figs. 3a and b given in Ref. [16], it is seen that the results are the same.

Lastly, we discuss the propagation characteristic of stress waves in isotropic fluid-saturated porous media. In calculation, we set $C_{11}=C_{22}=C_{33}=39.4\,\text{GPa}$, $C_{12}=C_{13}=C_{23}=5.8\,\text{GPa}$, $C_{44}=C_{55}=C_{66}=(C_{11}-C_{12})/2=16.8\,\text{GPa}$, $k_1=k_2=k_3\,600\,\text{mD}$, $T_1=T_2=T_3=2\,\text{mD}$, while the other parameters are the same as those listed in Table 1. The results shown that there are two kinds of longitudinal waves: fast wave, marked as 'L1', and slow wave, marked as 'L2'; and one kind of transverse wave, marked as 'S'. In any plane, the velocity curves and wave fronts are all circles and coincide with each other. It is similar to the situation of wave propagation in isotropic pure solids [15].

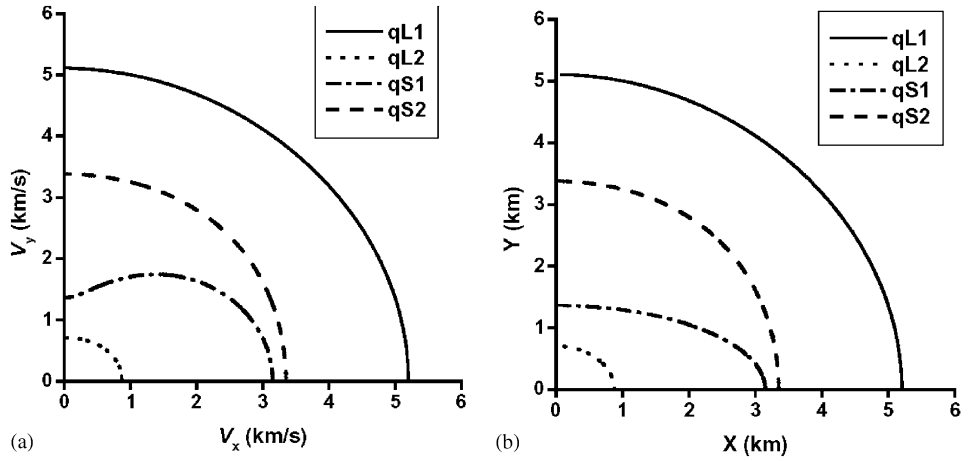

Fig. 3. (a) Velocity surface in the plane xOy for orthotropic fluid-saturated porous media. (b) Velocity surface in the plane xOy for orthotropic fluid-saturated porous media.

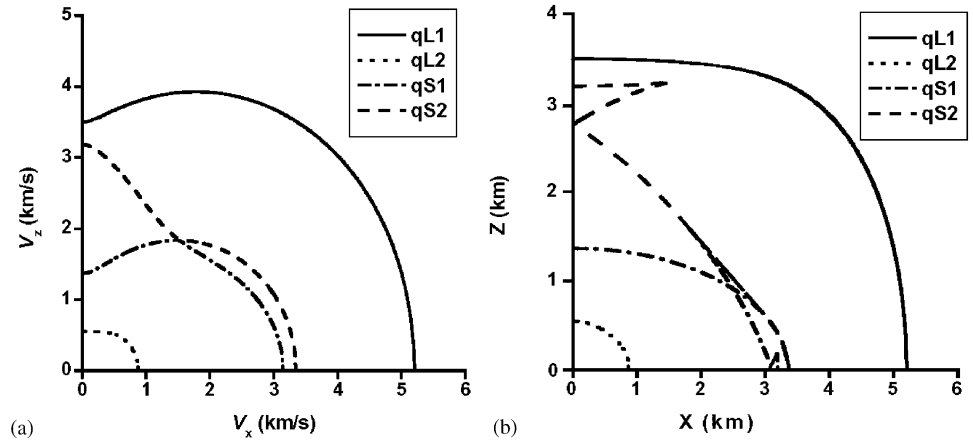

Fig. 4. (a) Velocity surface in the plane xOz for orthotropic fluid-saturated porous media. (b) Wave fronts in the plane xOz for orthotropic fluid-saturated porous media.

6. Conclusions

Summarizing the results above, we assert that the discussion about the velocity surfaces and wave fronts in the orthotropic fluid-saturated porous media and its special cases is helpful to disclose some basic characteristic and phenomena of waves in anisotropic fluid-saturated porous media. In isotropic fluid-saturated porous media or the iso-plane of transversely isotropic porous media, the velocity surfaces and wave fronts are circles and coincide with each other. In orthotropic fluid-saturated porous media or in the aniso-plane of transversely isotropic

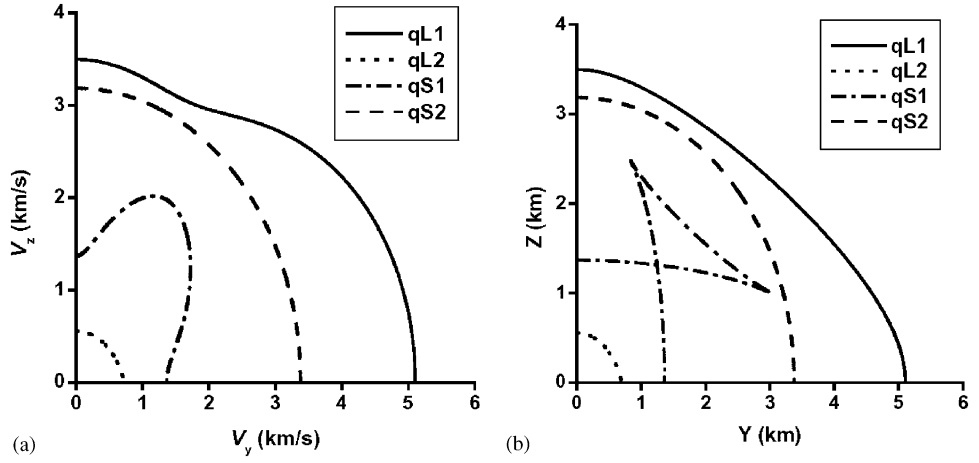

Fig. 5. (a) Velocity surface in the plane yOz for orthotropic fluid-saturated porous mediia. (b) Wave fronts in the plane yOz for orthotropic fluid-saturated porous media.

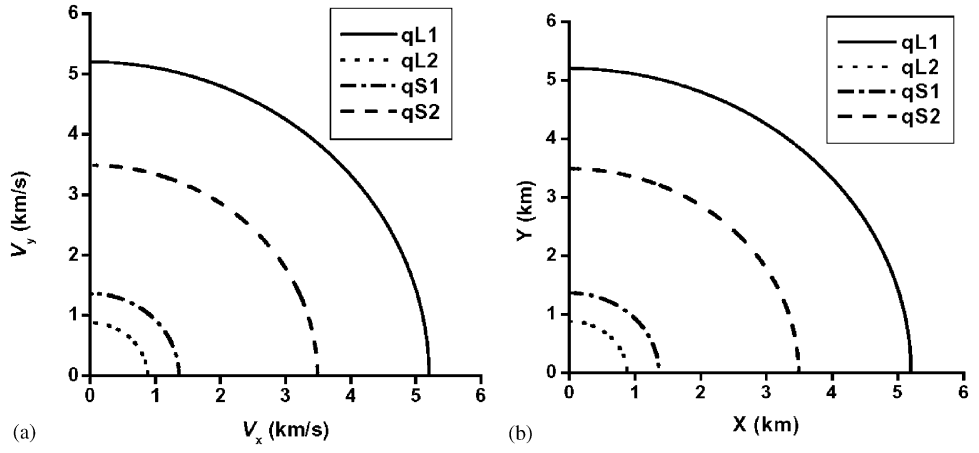

Fig. 6. (a) Velocity surface in the iso-plane xOy for orthotropic fluid-saturated porous mediia. (b) Wave fronts in theiso- plane xOz for orthotropic fluid-saturated porous media.

fluid-saturated porous media, along with the increase of anisotropy of the media, the velocity surfaces and wave fronts gradually change from circles to irregular shapes, and more than one triple angle may appear on the wave fronts when anisotropy is great. The slow wave has almost the same properties as the fast wave. They are both less sensitive to anisotropy of the media. The characteristic analysis results obtained in this paper also show that the generalized characteristic theory is an effective and accurate means for investigating the features of stress wave propagation in anisotropic fluid-saturated porous media.

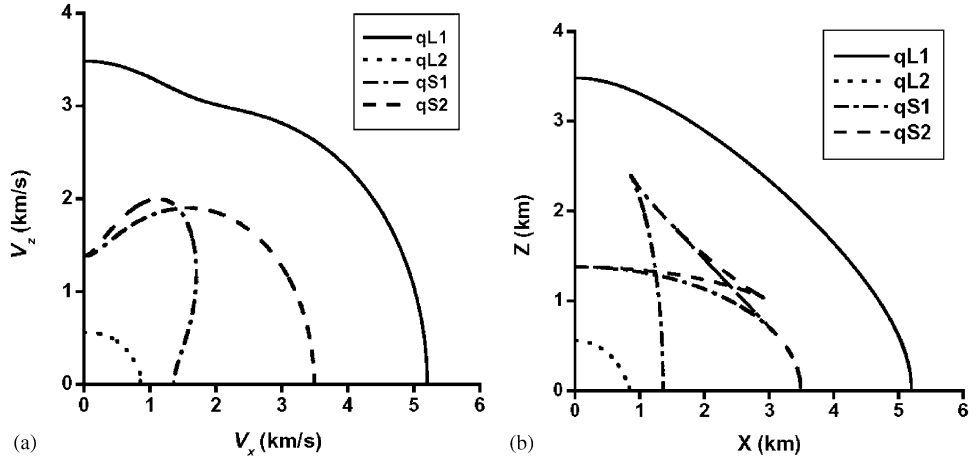

Fig. 7. (a) Velocity surface in the aniso-plane xOz for transversely istropic fluid-saturated porous media. (b) Wave fronts in the aniso-plane xOz for transversely isotropic fluid-saturated porous media.

Acknowledgements

The authors gratefully acknowledge the financial support of the National Natural Science Foundation of China and the support of Hong Kong RGC Grant HKUST6079/00E.

References

[1] M.A. Biot, Theory of elastic waves in a fluid-saturated porous solid, I. low frquency range, *Journal of the Acoustical Society of America* 28 (1956) 168–178.
[2] M.A. Biot, Theory of elastic waves in a fluid-saturated porous solid, II. High frequency range, *Journal of the Acoustical Society of America* 28 (1956) 179–191.
[3] M.A. Biot, Mechanics of deformations and acoustic propagation in porous media, *Journal of Applied Physics* 33 (1962) 1482–1489.
[4] M.A. Biot, Generalized theory of acoustic propagation in porous dissipative media, *Journal of the Acoustical Society of America* 34 (1962) 1254–1264.
[5] T.J. Plona, Observation of a second bulk compressional wave in porous medium at ultrasonic frequencies, *Applied Physics Letters* 36 (1980) 259–261.
[6] J.L. Auriault, L. Borne, R. Chambon, Dynamics of porous saturated media. Checking of the generalized law of dary, *Journal of the Acoustical Society of America* 77 (1985) 1641–1950.
[7] D.L. Johnson, Theory of dynamic permeability and tortuosity in fluid-saturated porous media, *Journal of Fluid Mechanics* 176 (1987) 379–402.
[8] M. Tajuddin, S.L. Ahmed, Dynamic interation of a poroelastic layer and a half-space, *Journal of the Acoustical Society of America* 89 (1991) 1169–1175.
[9] P.D. Schmitt, Acoustic multipole logging in transversely isotropic poroelastic formation, *Journal of the Acoustical Society of America* 86 (1989) 2397–2421.
[10] M.D. Sharma, M.L. Gogna, Wave propagation in anisotropic liquid-saturated porous solids, *Journal of the Acoustical Society of America* 90 (1991) 1068–1073.

[11] Y. Liu, K. Liu, S. Tanimura, Wave propagation in transversely isotropic fluid-saturated poroelastic media, *JSME International Journal* 45 (2002) 348–355.
[12] K. Liu, Y. Liu, Rayleigh waves in orthotropic fluid-saturated porous media, *Journal of Sound and Vibration* 271 (2004) 1–13.
[13] K. Liu, Y. Liu, Characteristic analysis for Rayleigh waves in transversely isotropic fluid-saturated porous media, *Acta Mechanica Sinica* 35 (2003) 100–104 (in Chinese).
[14] J.M. Carcione, *Wave Fields in Real Media: Wave Propagation in Anisotropic, Anelastic and Porous Media*, Elsevier, Amsterdam, 2001.
[15] T.C.T. Ting, *Nonlinear Waves in Solids*, Chinese Friendship Press, Beijing, 1981 (in Chinese).
[16] J.M. Carcione, Wave propagation in anisotropic. Saturated porous media: plane wave theory and numerical simulation, *Journal of the Acoustical Society of America* 99 (1996) 2655–2666.
[17] T.C.T. Ting, Characteristic forms of differential equations for wave propagation in nonlinear media, *Journal Applied Mechanics* 48 (1981) 743–748.
[18] B.R. Simon, D.K. Paul, An analytical solution for the transversely isotropic poroelastic formations, *Journal of the Acoustical Society of America* 86 (1989) 2397–2421.
[19] C.M. Francis, Wave surfaces due to impact on anisotropic plates, *Journal of Composite Materials* 6 (1972) 62–79.
[20] B.A. Auld, *Acoustic Fields and Waves in Solids*, Krieger, Florida, 1989.